Rab10 associates with primary cilia and the exocyst complex in renal epithelial cells

Clifford M. Babbey, Robert L. Bacallao and Kenneth W. Dunn

Am J Physiol Renal Physiol 299:F495-F506, 2010. First published 24 June 2010;
doi: 10.1152/ajprenal.00198.2010

Am J Physiol Renal Physiol 299: F495–F506, 2010.
First published June 24, 2010; doi:10.1152/ajprenal.00198.2010.

Rab10 associates with primary cilia and the exocyst complex in renal epithelial cells

Clifford M. Babbey, Robert L. Bacallao, and Kenneth W. Dunn

Department of Medicine, Division of Nephrology, Indiana University Medical Center, Indianapolis, Indiana

Submitted 6 April 2010; accepted in final form 21 June 2010

Babbey CM, Bacallao RL, Dunn KW. Rab10 associates with primary cilia and the exocyst complex in renal epithelial cells. *Am J Physiol Renal Physiol* 299: F495–F506, 2010. First published June 24, 2010; doi:10.1152/ajprenal.00198.2010.—Rab10, a mammalian homolog of the yeast Sec4p protein, has previously been associated with endocytic recycling and biosynthetic membrane transport in cultured epithelia and with Glut4 translocation in adipocytes. Here, we report that Rab10 associates with primary cilia in renal epithelia in culture and in vivo. In addition, we find that Rab10 also colocalizes with exocyst proteins at the base of nascent cilia, and physically interacts with the exocyst complex, as detected with anti-Sec8 antibodies. These data suggest that membrane transport to the primary cilum may be mediated by interactions between Rab10 and an exocyst complex located at the cilium base.

primary cilium; Sec8

THE PRIMARY CILIUM, ONCE RELEGATED as a biological curiosity, has come to be appreciated as a fundamentally important cellular organelle, involved in cell signaling and critical to tissue development in multicellular organisms (61). The significance of the cilium is demonstrated by the range of disorders that have come to be called "ciliary diseases," such as polycystic kidney disease, Bardet-Biedl syndrome, retinitis pigmentosa, Meckel-Gruber syndrome, and oral-facial-digital syndrome (40).

The mechanism by which cilia affect development appears to involve crucial signaling processes that depend on presentation of specific membrane proteins on the surface of the cilium. For example, the cilium is highly enriched in proteins associated with Hedgehog signaling, which depends on transport of Smoothened to the primary cilium following receptor binding (14, 56). Platelet-derived growth factor (PDGF) signaling depends on expression of PDGF receptor alpha on cilia of growth-arrested cells (62). Flow-dependent calcium signaling in epithelia depends on localization of polycystin-1 and polycystin-2 on the primary cilium (47). G protein signaling in neurons depends on ciliary localization of G protein-coupled receptors (4). While an extensive literature describes the molecular components of transport within the cilium (63), less is known about the crucial process by which membrane proteins are targeted and transported to the primary cilium.

Although a recent study demonstrates that ciliogenesis in mammalian epithelia depends on a set of proteins associated with transport to the apical plasma membrane (68), an increasing number of studies have associated transport to the cilium with proteins of the exocyst complex. Originally identified in yeast as a complex of proteins mediating docking and fusion of transport vesicles at the site of the forming bud (45), the exocyst has since been found to mediate membrane transport and morphogenesis in a broad range of eukaryotes, from plants to invertebrates to humans. In mammalian cells, the exocyst was originally associated with traffic to the basolateral plasma membrane in epithelial cells (21, 77). However, morphological studies have also associated the exocyst proteins with the primary cilium of Madin-Darby canine kidney (MDCK) cells (55) and functional studies demonstrated that Sec10 is necessary for ciliogenesis (81). Proteomic analysis associated nearly every exocyst protein with the mouse photoreceptor sensory cilium (38). Rab8, a mammalian homolog of the yeast Sec4p exocyst-associated protein, has also been associated with the primary cilium (16, 35, 42, 46, 79). Taken together, these studies suggest an attractive model in which membrane transport to the primary cilium of mammalian cells is mediated by protein interactions with the exocyst complex.

We and others previously showed that Rab10, another mammalian homolog of Sec4p, mediates membrane transport to the basolateral membrane of MDCK cells (3, 64) and intestinal epithelia of C. elegans (10). Here, we show that Rab10 also associates with the primary cilium and with the basal body of nascent cilia of renal epithelia. In addition, we show that Rab10 colocalizes with the exocyst proteins Sec6 and Sec8 at the cilium basal body, and physically interacts in a protein complex with Sec8.

MATERIALS AND METHODS

Cell culture. Studies were conducted using PTR cells, MDCK strain II cells transfected with both the human TfR and the rabbit polymeric immunoglobulin receptor (pIgR), as previously described (3, 5, 70, 71).

PTR cells were grown in MEM (Life Technologies, Grand Island, NY) with 8% FBS, 1% L-glutamine, streptomycin, and 0.05% hygromycin (Calbiochem, San Diego, CA). Cells were passed every 3 to 4 days and growth medium was changed daily. New cultures of cells were thawed every 4–5 wk. For fluorescence experiments, cells were plated either on coverslip-bottomed 35-mm dishes (Mattek, Ashland, MA) or plated at confluence on the bottoms of collagen-coated Millipore CM 12-mm filters and cultured for 4–5 days before experiments, as described previously (3, 5, 70, 71).

Antibodies to Rab10. Antibodies against Rab10 were raised using rabbit as a host (Open Biosystems). Two epitopes were identified for antibody preparation (EDILRKTPVKEPNSENVD and SKWLRNIDEHANEDVER), both targeting regions completely conserved across canine, mouse, rat, and human. As described below, both antibodies (referred to as EDI and SKW in the text) provided effective, specific detection of Rab10 via both immunofluorescence and immunoblotting.

Plasmids and transient transfection. Amino terminal eGFP chimeras of mutant and wild-type Rab10 were produced as described previously (3). The pEGFP-rab11 plasmid is as described previously (71). Plasmid encoding eGFP-rab7 was obtained from A. Wandinger-

Address for reprint requests and other correspondence: K. Dunn, Dept. of Medicine, Div. of Nephrology, Indiana Univ. Medical Center, Indianapolis, IN 46202 (e-mail: kwdunn@iupui.edu).

Ness (Univ. of New Mexico). Plasmid encoding FLAG epitope-tagged Rab10 was obtained from B. Grant (Rutgers Univ.). shRNA plasmids were constructed to transiently knockdown expression of Rab10. Four target sequences were selected using publically available tools (Invitrogen) and targeted against the canine sequence [*1*) GGAGCAATGGGTATCATGC, *2*) GGAAAAGGAGAGCAGATTG, *3*) GGGAGCATGGTATTAGATT, *4*) GACAGGCTGGAAGAGCAAATG]. Complementary oligonucleotides were synthesized, annealed, and directionally cloned into the pDsiPHER-GFP plasmid (Molecula) using *Hin*dIII/*Bam*HI sites.

Cells were transfected immediately following seeding onto filters, or the day following plating onto coverslip-bottomed dishes using GeneJammer transfection agent from Stratagene (La Jolla, CA), per manufacturer's protocol. A ratio of 2.8 μl transfection agent to 0.8 μg plasmid DNA was found to be optimal.

Proteins and chemicals. Human transferrin (Tf) was obtained from Sigma, iron loaded and purified as described in Ref. 75, and conjugated to TexasRed (TxR; Invitrogen) as described previously (3, 5, 70, 71). Antibody against acetylated tubulin was obtained from Santa Cruz Biotechnology, antibodies against Sec6 and Sec8 were obtained from Stressgen Biotechnologies, antibody against the FLAG epitope was obtained from Sigma, and antibody against Rab8 was obtained from BD Transduction Laboratories. All secondary antibodies and OregonGreen Phalloidin were obtained from Invitrogen.

Immunofluorescence. As described in RESULTS, two different procedures were used for immunofluorescence localization of proteins. In our standard protocol, cells are washed in PBS at 37°C and then fixed in 4% fresh paraformaldehyde for 15 min at room temperature. Remaining unreacted paraformaldehyde is quenched with three washes in 100 mM glycine in PBS for 15 min. Cells are then permeabilized in a solution of 0.2% saponin, 4% BSA in PBS (blocking buffer) for 15 min. Cells are then incubated with primary antibody in blocking buffer for 1 h at room temperature, rinsed in three changes of blocking buffer over 15 min, and then incubated with secondary antibody in blocking buffer for 1 h at room temperature, followed by another rinse in three changes of blocking buffer over 15 min. In one study (see Fig. 5, *A*-*C*), cells were incubated with primary antibody overnight at 4°C. Cells were then transferred to PBS with 2% DABCO for microscopy. In the second immunofluorescence procedure, cells are first rinsed in PBS at 37°C, prepermeabilized in a solution of 0.01% saponin, 4% BSA in PBS for 60 s, and then rinsed again in PBS. Cells are then processed as per the standard protocol above.

For immunofluorescence of mouse and rat tissue, kidneys were perfusion fixed with 4% paraformaldehyde, and 150-μm slices were prepared via microtome. Tissue slices were rinsed in multiple changes of PBS over a period of 24 h at room temperature in a shaker bath. Tissues were then incubated with Rab10 antibody in blocking buffer (0.05% Triton X-100, 2% BSA in PBS) for 24 h with agitation. Tissues were then washed three times with blocking buffer for 1 h each and then incubated with secondary antibody for 24 h with agitation. Tissues were then washed three times with blocking buffer for 1 h each, postfixed in 4% fresh paraformaldehyde for 30 min, washed in 100 mM glycine in PBS for 15 min, and then three times in PBS for 10 min each. All procedures were carried out in accordance with the National Institutes of Health *Guide for the Care and Use of Laboratory Animals*, and protocols were approved by the Indiana University School of Medicine Animal Care and Use Committee.

Labeling of cells with fluorescent Tf. Cells were incubated at 37°C on a slide warmer in a humidified chamber for 15 min and then for an additional 20 min with 20 μg/ml TxR-labeled Tf (TxR-Tf). Incubations were conducted in *medium 1* (150 mM NaCl, 20 mM HEPES, 1 mM $CaCl_2$, 5 mM KCl, 1 mM $MgCl_2$, 10 mM glucose, pH 7.4). After incubation, filters were rinsed briefly in PBS at 4°C and then fixed with 4% paraformaldehyde in pH 7.4 PBS at 4°C for 15 min. Filters were then rinsed in PBS. The specificity of receptor-mediated uptake of fluorescently labeled Tf was previously demonstrated (3, 5, 70, 71).

Microscopy. Analyses of MDCK cells were conducted using a Perkin-Elmer Ultraview confocal microscope system mounted on a Nikon TE 2000U inverted microscope, using Nikon ×60 NA 1.2 water immersion or Nikon ×100 NA 1.4 oil immersion planapochromatic objectives. The system is equipped with an Andor EM-CCD system (South Windsor, CT). Image volumes were collected by collecting a vertical series of images, each between 0.2 and 0.6 μm apart.

For microscopy of filter-grown cells, cells were grown on the underside of Millipore filter units. After the legs of the filter units were removed, living or fixed cells were observed by placing the entire filter unit on two 50-μm tape spacers attached to the coverslip of a coverslip-bottomed 35-mm dish (Mattek) mounted on the stage of an inverted microscope. For live cell studies, incubations are conducted in *medium 1* on the microscope stage. Temperature is maintained with a microscope stage heater, using Warner Instruments TC324B (Hamden, CT).

Microscopy of mouse and rat kidney tissue was conducted using a Bio-Rad MRC1024 confocal microscope mounted on a Nikon Eclipse 200, using a ×60 NA 1.2 water immersion planapochromatic objective, with the exception of the image shown in Fig. 2*D*, which was collected using the PerkinElmer system described above.

Image processing. Image processing was conducted using Metamorph software (Universal Imaging, West Chester, PA). For images with poor signal-to-noise, images were subsequently averaged spatially using a 3 × 3 Gaussian filter. Images shown in figures were contrast stretched to enhance the visibility of dim structures, and specific care was taken never to enhance the contrast in such a way that dim objects were deleted from an image. Images to be compared were always contrast enhanced identically. Montages were assembled and annotated using Photoshop (Adobe, Mountain View, CA). Volume renderings were conducted using Voxx, a PC-based image analysis program developed and distributed freely by the Indiana Center for Biological Microscopy (Clendenon et al., 2002; http://nephrology.iupui.edu/imaging/voxx).

Immunoblotting and immunoprecipitation. PTR cells were plated at 75% confluence on 100-cm Petri dishes. Cells were harvested for analysis 4 days after they reached confluence. Cells were washed twice with ice-cold PBS supplemented with 0.5 mM $CaCl_2$ and $MgCl_2$ (PBS+). After the final wash, the cells were scraped in a total volume of 1.5 ml PBS+ and centrifuged at 600 *g* for 5 min at 4°C. Cell pellets were resuspended in 250 μl 20 mM sucrose, 150 mM NaCl, 20 mM Tris·HCl, pH 7.5, 2 mM $MgCl_2$, 5 mM $CaCl_2$ supplemented with protease inhibitors (Sigma, St. Louis, MO) and 2 mM GTP-γS (Sigma; *buffer A*). The suspension was passed eight times through a precooled ball-bearing homogenizer (Stanford University, Stanford, CA). The samples were collected and centrifuged at 600 *g* to remove nuclei and large cellular debris. Supernatants were sonicated with a Branson model 450 Sonifier (VWR Scientific, West Chester, PA), equipped with a microprobe to shear the DNA. Samples were flash-frozen in liquid nitrogen and stored at −80°C for later use. Protein concentration of all lysates was measured using the BCA protein assay kit from Thermo Scientific (Rockford, IL).

In all immunoprecipitations performed for this study, 100 μg of lysate were used as starting material. *Buffer A* was added to bring the total volume to 250 μl. Either 9 μg of affinity-purified anti-Rab10 or 1.5 μl each of the following monoclonal anti-sec 8 antibodies (5C3, 2E12, 1002) were added to samples. Equivalent volume of preimmune antibody was added to samples as a control for Rab10 immunoprecipitation experiments. Alternatively, Rab10 antibody was preincubated with a 10-fold molar excess of immunizing peptide for 60 min before addition to lysates. Antibodies were added to samples and incubated at 37°C for 60 min under continuous agitation. Protein A beads (Dynabeads, Invitrogen, Carlsbad, CA) were added to all samples and incubated for 30 min at 37°C. Serial washes were performed with 1 ml of 150 mM NaCl, 20 mM Tris·HCl, pH 8.0, 1% Triton X-100, 500 mM NaCl, 20 mM Tris·HCl, pH 8.0, and 150 mM

NaCl, 20 mM Tris·HCl, pH 8.0 after magnetic separation of beads. After the final wash, beads were centrifuged and resuspended in 150 mM NaCl, 20 mM Tris·HCl, pH 8.0 and an equal volume of 2× sample buffer with 50 mM DTT was added to each sample. After samples were heated at 70°C for 10 min, samples were briefly centrifuged. Equivalent volumes of each sample were loaded using a Hamilton syringe and samples were run on 4–12% gradient gels (NuPage, Invitrogen). Proteins were transferred to nitrocellulose for immune blots and blots were incubated with either goat anti-Rab10 (Santa Cruz Life Sciences, Santa Cruz, CA) or mouse monoclonal anti-Sec8 (8f12, generously provided by C. Yeaman, Univ. of Iowa) followed by incubation with donkey anti-goat IgG conjugated to horseradish peroxidase (HRP; Jackson Immuno Research, West Grove, PA).

RESULTS

Immunofluorescence localization of Rab10 on primary cilia of renal epithelial cells. We generated two rabbit polyclonal antibodies against Rab10, both targeting a region that is completely conserved across canine, mouse, rat, and human proteins (see MATERIALS AND METHODS). An example of the results of immunofluorescence studies using the EDI antibody is presented in Fig. 1, which shows a field of polarized MDCK cells, one of which expresses GFP-Rab10 (Fig. 1*A*). The specificity of the antibody is indicated by the fact that while all cells in the field show a punctate immunofluorescence (Fig. 1*B*) characteristic of Rab10 in endosomes, the fluorescence is much stronger in the compartments containing GFP-Rab10. The specificity of the EDI antibody is also indicated in immunoblots, which detected a band at the predicted molecular weight of ~22.5 kDa, a band that was compatible when antibody was preincubated with immunizing peptide (Supplementary Fig. 1; the online version of this article contains supplemental data). Expression of shRNA targeting Rab10 was found to decrease the amount of Rab10 detected by immunofluorescence or by immunoblotting (Supplementary Fig. 1). In contrast, levels of Rab8 were unaffected, demonstrating the absence of cross-reactivity of the Rab10 antibody with the closely related Rab8.

Unexpectedly, we observed that the anti-Rab10 antibody also labeled what appeared to be primary cilia extending from the cell apices (arrows in Fig. 1*C*). Anti-Rab10 antibody labeling of cilia is generally more apparent in projected *xz* sections (Fig. 1*D*), particularly when viewed as an animated volume rendering (*animation 1*). Cells shown in Fig. 1, *A–D*, were prepermeabilized with 0.01% saponin for 1 min before fixation, a procedure that has been found to enhance labeling of intracellular exocyst complex proteins (48) and appears to facilitate endosomal labeling. However, similar results are found using a conventional approach in which wells are permeabilized following fixation (Fig. 1*G*). Dual immunofluorescence studies in which cells were immunolabeled for both Rab10 (Fig. 1*E*) and acetylated tubulin (Fig. 1*F*), a marker of primary cilia, confirmed the identity of the Rab10-labeled primary cilium. Control studies in which cells were labeled with preimmune serum showed no cytosolic or ciliary Rab10 labeling (Fig. 1, *H* and *I*). Immunofluorescence studies with the second (SKW)Rab10 antibody likewise detected Rab10 on primary cilia (Supplementary Fig. 1).

Ciliary Rab10 was also found in immunofluorescence studies of mouse kidney tissue. For these studies, phalloidin was used to label filamentous actin, enabling identification of proximal tubules on the basis of their actin-rich brush borders. As shown in Fig. 2, both the EDI (Fig. 2, *A–C*) and SKW Rab10 antibodies (Fig. 2, *E–G*) label both cytosolic structures and cilia extending into the lumen of distal tubules in mouse kidney tissue. We find no evidence of immune-labeled cilia in proximal tubule cells (Fig. 2, *A–C*, *insets*) nor in vascular tissue (Fig. 2*H*).

Similar results were obtained in immunofluorescence studies of rat kidney tissue (Fig. 2, *I–L*). As was found in studies of mouse tissue, Rab10 antibodies again label cilia extending into the lumen of distal but not proximal tubules (compare distal

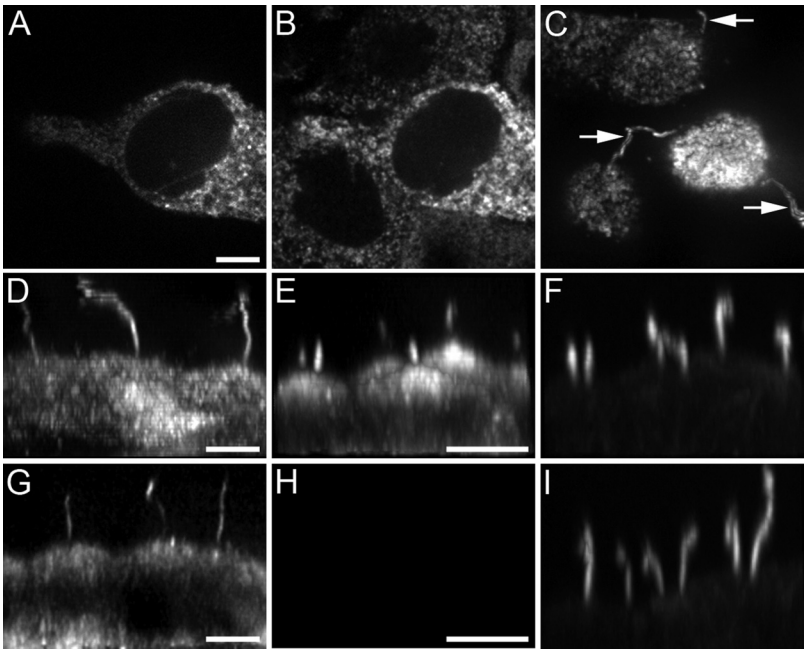

Fig. 1. EDI Rab10 antibody labels primary cilia in Madin-Darby canine kidney (MDCK) cells. *A*: medial image plane collected from a field of MDCK cells, one of which expresses GFP-Rab10. *B*: distribution of anti-Rab10 in the same field, showing that the Rab10 antibody colocalizes on intracellular structures associated with GFP-Rab10. As expected, immunofluorescence is weaker in cells that express only endogenous levels of Rab10. *C*: projected image of focal planes at and above the tops of the cells shows that the Rab10 antibody also recognizes cilia extending from the apical membrane. *D*: apical extension of the cilia is more obvious in the *xz* projection of cells labeled with anti-Rab10 antibody. This same volume is presented as an animated volume rendering (*animation 1* in Supplementary Material). *G*: as in *D*, but cells were fixed before permeabilization. Similar results are obtained by either method. *E* and *F*: *xz* projections of anti-Rab10 and anti-acetylated tubulin immunofluorescence, respectively, verify that the apical projections labeled with anti-Rab10 antibody are primary cilia. *H* and *I*: as in *E* and *F*, except that preimmune serum was used in place of anti-Rab10 antibody (*H*). Scale bars = 10 μm in length.

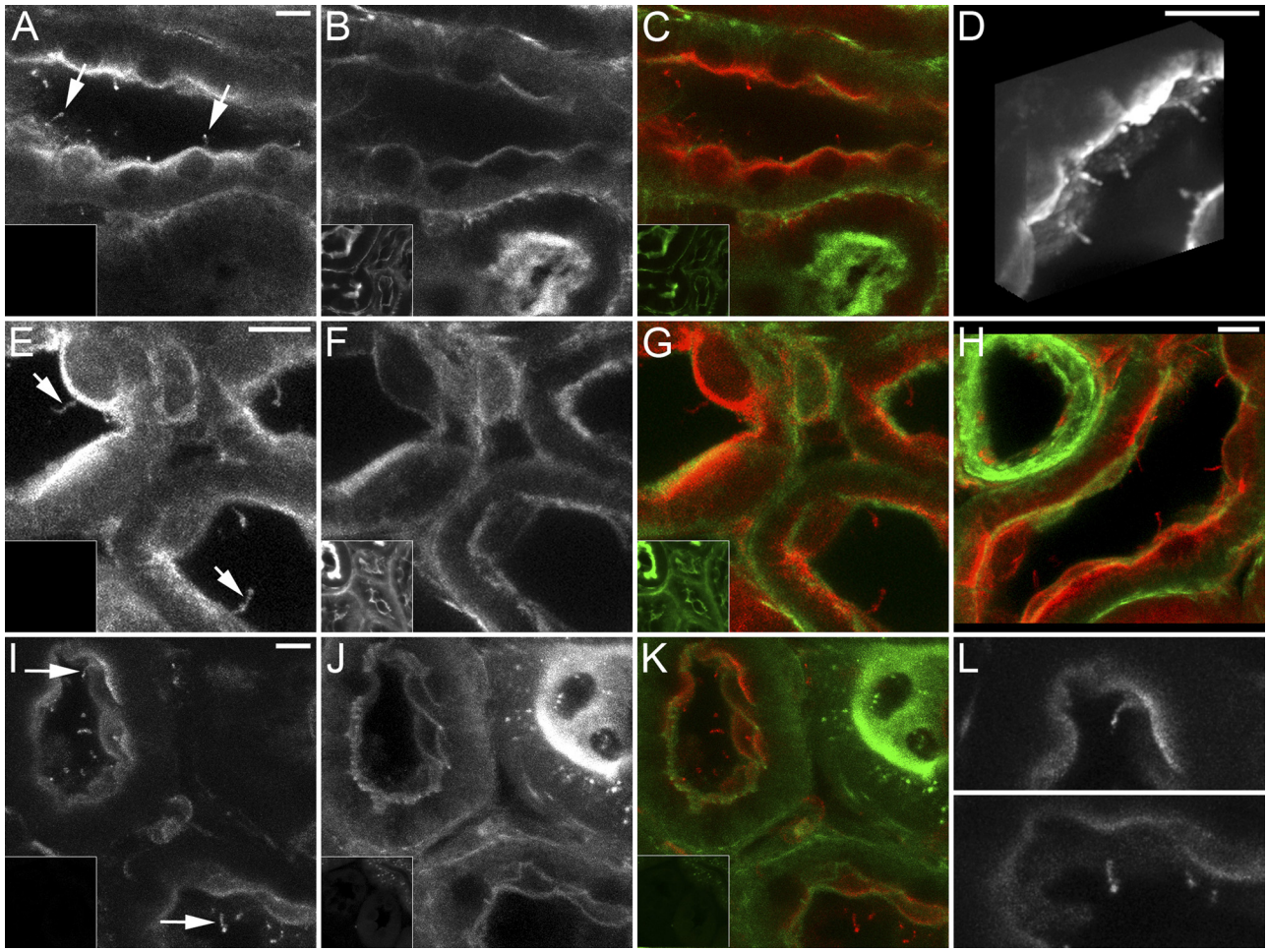

Fig. 2. Both EDI and SKW Rab10 antibodies label primary cilia in rodent renal tubules. *A*: projected image volume of EDI anti-Rab10 immunofluorescence in fixed mouse kidney tissue. *B*: Oregon Green-Phalloidin fluorescence in the same volume shown in *A*. *C*: color merge of anti-Rab10 (red) and Oregon Green-Phalloidin (green) shown in *A* and *B*. Note the absence of ciliary Rab10 in proximal tubule cells, as identified by their actin-rich brush border (*bottom right*). *Insets* in these and following images show tissues labeled with phalloidin and preimmune serum in place of Rab10 antibody. *D*: volume rendering of EDI anti-Rab10 immunofluorescence in mouse renal tubule. This same volume is presented as an animated volume rendering (*animation 2* in Supplementary Material). *E*: projected image volume of anti-Rab10 immunofluorescence in fixed mouse kidney tissue, using the SKW anti-Rab10 antibody. *F*: Oregon Green-Phalloidin fluorescence in the same volume shown in *E*. *G*: color merge of anti-Rab10 (red) and Oregon Green-Phalloidin (green) shown in *E* and *F*. *H*: color merge of EDI anti-Rab10 (red) and Oregon Green-Phalloidin (green) in fixed mouse kidney tissue, showing the absence of ciliary Rab10 in vasculature (*top left*). Renderings shown in *G* and *H* are presented together in an animated volume rendering (*animation 3* in Supplementary Material). *I*: projected image volume of anti-EDI Rab10 immunofluorescence in fixed rat kidney tissue. *J*: Oregon Green-Phalloidin fluorescence in the same volume shown in *I*. *K*: color merge of anti-Rab10 (red) and Oregon Green-Phalloidin (green) shown in *I* and *J*. As in the mouse tissues, note the absence of ciliary Rab10 in proximal tubule cells, as identified by their actin-rich brush border (*top right*). *L*: high-magnification images of 2 of the tubular regions shown in *I*. Scale bars = 20 μm in length.

tubules at *bottom left* with proximal tubule at *top right* in Fig. 2, *I–K*). Insofar as cilia appear at different depths, and project in different angles, they are more apparent in animated volume renderings than in static two-dimensional images. For this reason, the reader is encouraged to view *animation 2*, which shows an animated rendering of Rab10 immunofluorescence in mouse kidney tissue (Fig. 2*D*), and *animation 3*, which shows animated renderings of the image volumes shown in Fig. 2, *G* and *H*. Although we found no evidence of Rab10 on primary cilia of proximal tubule cells in rat or mouse tissue, the absence may reflect interference with the elaborate brush border developed in vivo as Rab10 was detected on primary cilia of LLC-PK1 cells, a cultured cell line derived from porcine renal proximal tubule cells (Supplementary Fig. 1).

GFP chimeras of Rab10 localize to the base of primary cilia. In previous studies from both our laboratory (3) and others (64), GFP chimeras of Rab10 were found to localize to endosomes and to the *trans*-Golgi network (TGN), with no obvious ciliary localization. In particular, we found that GFP-Rab10 colocalized almost completely with internalized Tf in polarized MDCK cells. Based on our observations that Rab10 immunolocalized to cilia, we revisited the question of whether GFP-Rab10 associates with cilia. As shown in Fig. 3, GFP-Rab10 (Fig. 3*A*) colocalizes almost completely with endosomes containing internalized Tf (Fig. 3*B*) in medial planes of polarized MDCK cells, consistent with our previous studies (3). However, inspection of *xz* projections in some cells shows short apical protuberances brightly labeled with GFP-Rab10 that lack internalized Tf. The limited distribution of GFP-Rab10 on the cilium shaft may reflect the transient expression system, as transiently expressing FLAG epitope-labeled Rab10 likewise associates with a short apical knob (Supplementary Fig. 2).

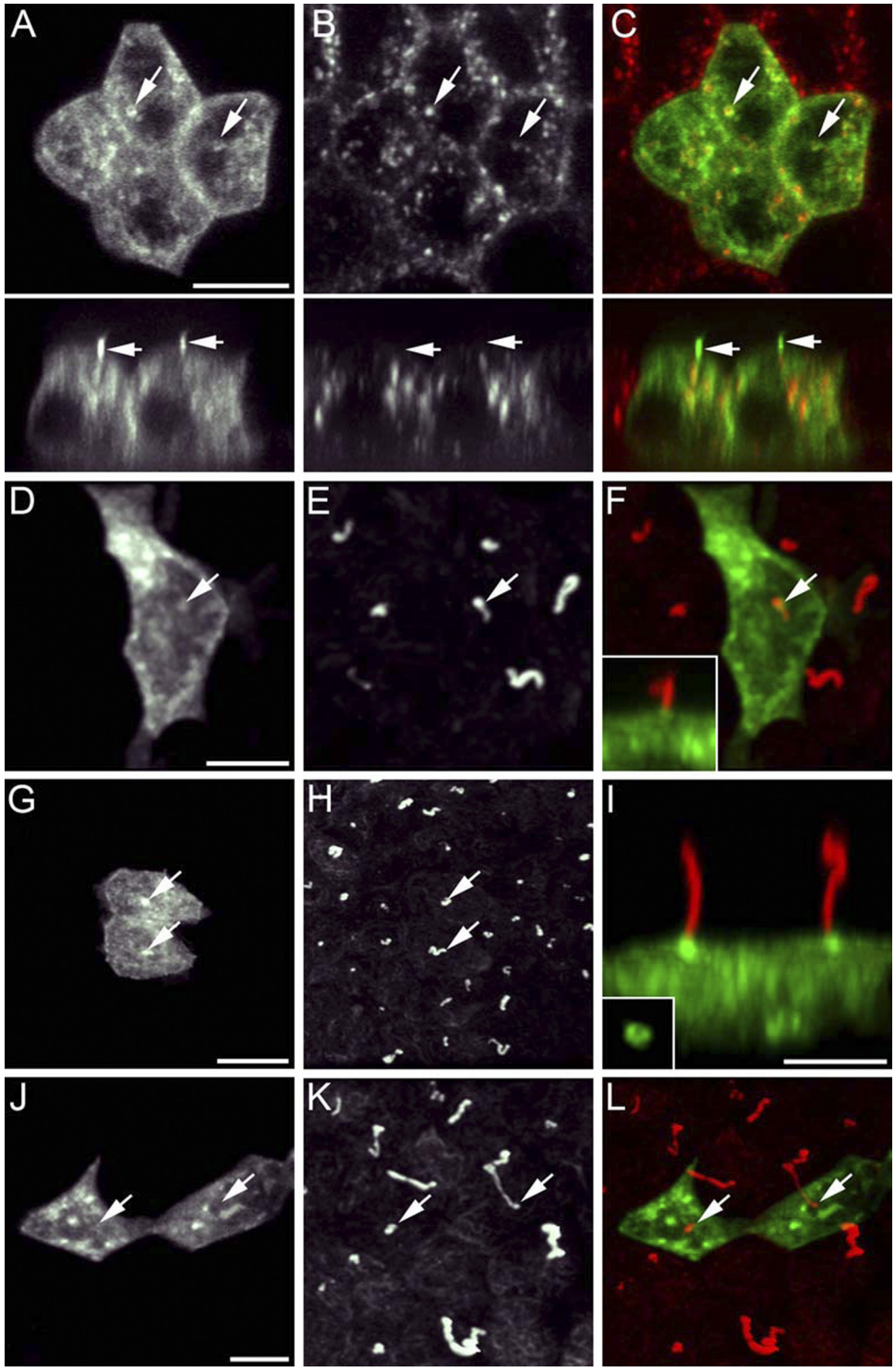

Fig. 3. Overexpressed GFP-Rab10 localizes at the base of primary cilia. *A*: image of a medial focal plane of a group of MDCK cells expressing GFP-Rab10. *Bottom*: *xz* section of the same field. *B*: image of internalized TexasRed transferrin (TxR-Tf) collected from the same regions in *A* in *xy* section (*top*) and *xz* section (*bottom*). *C*: color merge of GFP-Rab10 (green) and TxR-Tf (red) shown in *A* and *B*. Arrows in the *xy* sections indicate endosomes associated with GFP-Rab10 containing internalized TxR-Tf. Arrows in *xz* sections indicate short apical GFP-Rab10-labeled stalks that lack internalized TxR-Tf. *D*: image of MDCK cell expressing GFP-Rab10. *E*: image of anti-acetylated tubulin immunofluorescence collected from the same field. *F*: color merge of GFP-Rab10 (green) and anti-acetylated tubulin (red) from the image volumes shown in *D* and *E*. Arrow indicates accumulation of GFP-Rab10 at base of a primary cilium (see *xz* section in *F*). *G*: image of MDCK cell expressing GFP-Rab10-Q68L. *H*: image of anti-acetylated tubulin immunofluorescence collected from the same field. *I*: color merge of *xz* projections of GFP-Rab10-Q68L (green) and anti-acetylated tubulin (red) from the image volumes shown in *G* and *H*. Arrows in *G* and *H* indicate strong accumulation of GFP-Rab10-Q68L at the base of 2 primary cilia. *I*, *inset*: high magnification of one of the ring structures associated with GFP-Rab10-Q68L. Image volumes shown in *F* and *I* are presented together in an animated volume rendering (*animation 4* in Supplementary Material). *J*: image of MDCK cell expressing GFP-Rab7. *K*: image of anti-acetylated tubulin immunofluorescence collected from the same field. *L*: color merge of GFP-Rab7 (green) and anti-acetyated tubulin (red) shown in *J* and *K*. Arrows indicate bases of 2 cilia, lacking GFP-Rab7. Scale bars = 10 μm in length for all images, except for *G* and *H*, which is 20 μm in length. *I*, *inset*: 2×.

Dual labeled studies demonstrate that GFP-Rab10 localizes to the base of primary cilia, as labeled with antibody to acetylated tubulin (Fig. 3, *D–F*). While ciliary localization of GFP-Rab10 is not especially strong, we consistently find that a GFP chimera of the GTPase-defective mutant Rab10-Q68L localizes to a prominent apical spot (Fig. 3*G*) located at the base of primary cilia (Fig. 3*H*). The image volumes of cells expressing GFP-Rab10 and GFP-Rab10-Q68L (Fig. 3, *F* and *I*) are also shown as animated renderings in *animation 4*. In many cases, the GFP-Rab10-Q68L apical spot take the form of a ring (Fig. 3*I*, *inset*), a point to which we will return later.

The specificity of the association of GFP-Rab10 with the primary cilium is indicated by the fact that while we found that GFP-Rab8 associates with the primary cilium, consistent with previous studies (46), we find no ciliary labeling by GFP chimeras of Rab7 (Fig. 3, *JL*) or Rab4, Rab5, or Rab25 in transiently transfected MDCK cells (data not shown). Consistent with our previous studies showing that YFP-Rab10-Q68L

codistributes with CFP-Rab11 (3), we find that GFP-Rab11 associates with an apical ring located at the base of primary cilia, but does not label the ciliary axoneme (Supplementary Fig. 2).

Rab10 colocalizes with exocyst proteins in apical spots and rings before ciliogenesis. Interestingly, in freshly plated MDCK cells that have not yet formed cilia, we frequently find that the EDI Rab10 antibody labels prominent apical spots (Fig. 4, *A* and *B*), suggesting that Rab10 may associate with the centrosome before ciliogenesis. Closer inspection shows that these apical spots frequently take the form of rings (Fig. 4*C*). Once ciliogenesis has commenced, the prominence of the apical spots is diminished, and Rab10 begins to appear on the nascent cilium (Fig. 4, *D* and *E*, also see *animation 5*). Similar apical anti-Rab10 rings are also found in studies of freshly plated LLC-PK1 cells (Fig. 4*F*) and in MDCK cells labeled with the SKWanti-Rab10 antibody (data not shown).

Previous studies localized exocyst proteins to apical centrosomes (1) and primary cilia (55, 81) in MDCK cells. Given that Rab10 is a mammalian homolog of the yeast Sec4p protein, whose effector is the yeast exocyst complex, it might be predicted that the apical exocyst similarly serves as a mammalian effector of Rab10. Consistent with this, we find an enhanced association of the GTP-locked mutant Rab10-Q68L with the apical ring of MDCK cells (Fig. 3), whereas we find no association of the GTP-binding mutant Rab10-T23N with apical structures (data not shown). To determine whether the apical Rab10 structure might correspond to the apical exocyst, we immunofluorescently labeled MDCK cells with antibodies to both Rab10 and the exocyst protein Sec8. Examination of apical planes showed a close colocalization of anti-Rab10 (Fig. 5*A*) with anti-Sec8 in apical rings (Fig. 5*B*). As shown in Fig. 5*B*, *inset*, Sec8 antibody also prominently labeled a lateral band around the short, relatively unpolarized cells (imaged 4 days after plating), consistent with previous studies localizing exocyst proteins at or near tight junctions following cell-cell contact (21, 37, 55, 77). Results of a similar experiment are shown in Fig. 5*C*, which shows the close colocalization of anti-Rab10 (*top*) with anti-Sec8 (*middle*) in rings in the apical planes of MDCK cells.

As described above, the apical Rab10 ring becomes less prominent during the process of ciliogenesis, and Rab10 is increasingly distributed to the cilium. In cells imaged 5 days after plating, shown in Fig. 5, *D–F*, anti-Rab10 colocalizes with anti-Sec8 at the base of nascent cilia, indicated with arrows in the *xz* sections shown in Fig. 5*F*. The three-dimensional distributions of Rab10 and Sec8 are easier to appreciate in the animated rendering of this image volume, shown in *animation 6*.

Immunofluorescence studies of MDCK cells imaged 4 days after plating likewise show that Sec6 immunofluorescence is found not only in puncta and lateral membranes of MDCK cells (Fig. 5*G*) but also in a single, bright spot that colocalizes with anti-Rab10 (Fig. 5, *H–J*).

If the exocyst serves as an effector of Rab10, one would expect to see an enhanced association of the exocyst with the GTPase-defective Rab10-Q68L, which would have a more stable interaction with the exocyst. As shown earlier, consistent with that prediction, we find that GFP-Rab10-Q68L forms a more prominent spot at the apex of MDCK cells than does GFP-Rab10 (Fig. 3). In addition, the GTP-binding mutant GFP-Rab10-T23N does not associate with an apical compartment at all (data not shown). Immunofluorescence studies of MDCK cells 4 days after plating demonstrate that the prominent GFP-Rab10-Q68L apical spot colocalizes with anti-Sec8. As shown in Fig. 6, immunolocalized Sec8 distributes to both lateral membranes and single apical spots in MDCK cells (Fig. 6*A*), where it colocalizes with GFP-Rab10-Q68L (Fig. 6, *B* and *C*). When viewed at higher magnification, many of these spots take on the ringed form shown in previous figures (Fig. 6, *D*, *E*, and *F*). Consistent with previous studies (11, 22), we also find that Sec8 localizes to abscission sites in dividing cells (Fig. 6*G*). Interestingly, GFP-Rab10-Q68L colocalizes with Sec8 at these abscission sites, suggesting an additional Rab10-

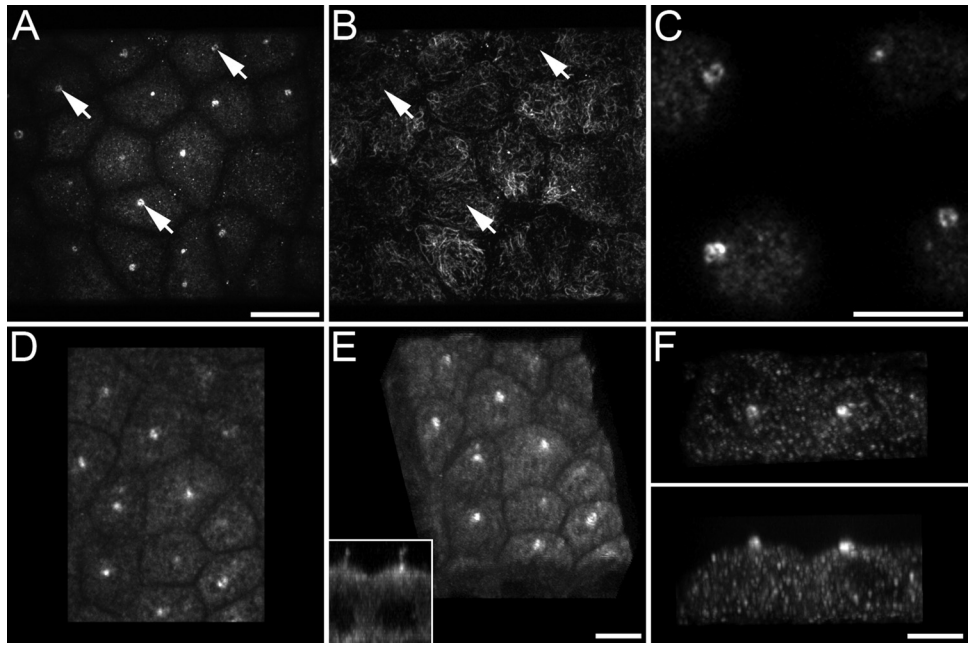

Fig. 4. Rab10 localizes to apical rings in MDCK and LLC-PK1 cells lacking cilia. *A*: projected image volume of EDI anti-Rab10 immunofluorescence in MDCK cells. *B*: image of anti-acetylated tubulin immunofluorescence in the same volume shown in *A*, showing the absence of primary cilia. *C*: higher-magnification image of cells shown in *A*, *top right*, showing that apical spots form ring structures. *D*: rendered image volume of EDI anti-Rab10 immunofluorescence in MDCK cells. *E*: rotated rendering showing apical localization of each anti-Rab10 spot. *E*, *inset*: *xz* projection of 2 cells from *top right* of field shown in *E*, showing anti-Rab10 labeling of nascent cilia in cells lacking apical Rab10 spots. This same volume is presented as an animated volume rendering (*animation 5* in Supplementary Material). *F*: projected image volume of EDI anti-Rab10 immunofluorescence in LLC-PK1 cells in *xy* (*top*) and *xz* (*bottom*) planes. Scale bars in *A* = 20 μm in length, remainder of scale bars are 10 μm in length.

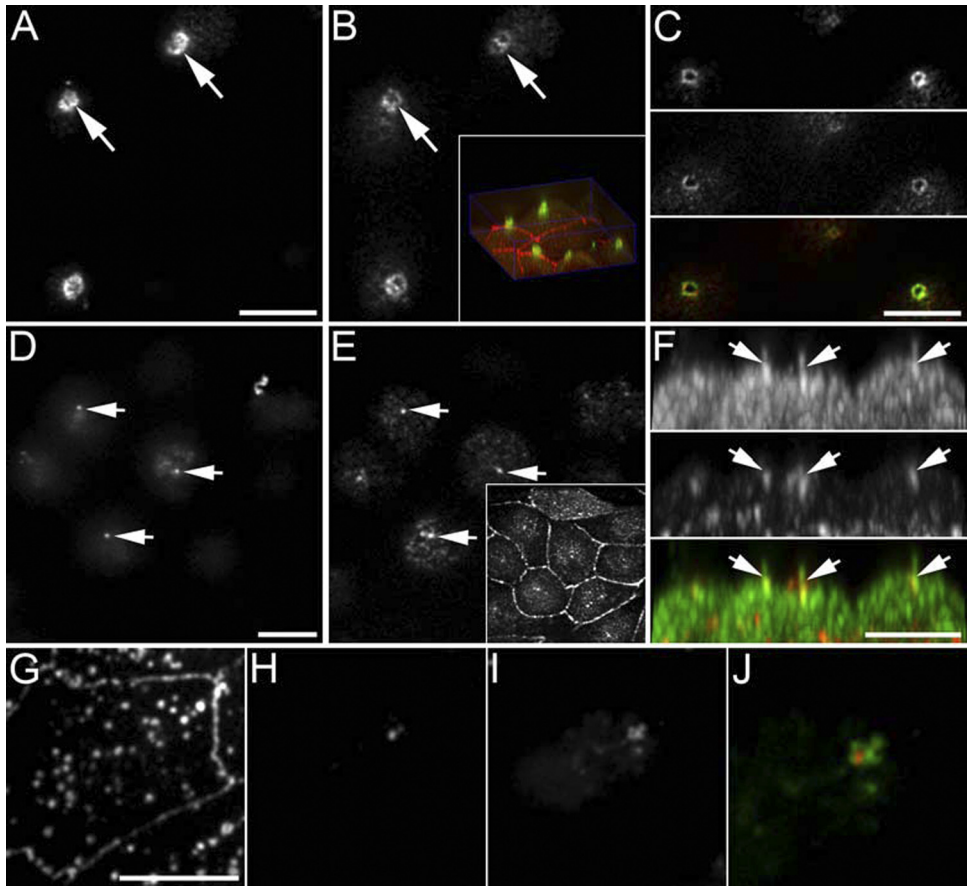

Fig. 5. Rab10 colocalizes with exocyst proteins in apical rings and at the base of nascent cilia. *A*: projected image of EDI anti-Rab10 immunofluorescence in apical planes of MDCK cells. *B*: projected image of anti-Sec8 immunofluorescence in the same image volume. Arrows indicate colocalization of Rab10 and Sec8 in apical ring structures. *B*, *inset*: tilted volume rendering of entire volume of cells, showing the apical localization of the Rab10-Sec8 structures, as well as the characteristic localization of Sec8 (red) at cell-cell junctions. *C*: projected image of EDI anti-Rab10 immunofluorescence (*top*) and Sec8 immunofluorescence (*middle*) in apical planes of another field of MDCK cells. *Bottom*: merged image of anti-Rab10 (green) and anti-Sec8 (red). *D*: projected image of EDI anti-Rab10 in apical planes of MDCK cells. Note that only the cell at *top right* shows labeling of Rab10 on extended cilium. *E*: projected image of anti-Sec8 immunofluorescence in the same image volume. Arrows indicate colocalization of Rab10 and Sec8 in apical rings/spots. *E*, *inset*: projected image of entire volume of cells, showing the characteristic localization of Sec8 at cell-cell junctions. *F*: *xz* sections of the anti-Rab10 (*top*) and anti-Sec8 (*middle*) from the same volume shown in *D* and *E*. Arrows indicate tops of spots labeled with both anti-Rab10 and anti-Sec8, from which short processes extend, labeled with Rab10 alone. *Bottom*: merged image of anti-Rab10 (green) and anti-Sec8 (red). The 3-dimensional distributions of FP-Rab10 and Sec8 are easier to appreciate in the animated rendering of this image volume, shown in *animation 6*. *G*: image of anti-Sec6 immunofluorescence collected from medial plane of MDCK cells, showing characteristic junctional localization of Sec6. *H*: projected image of anti-Sec6 immunofluorescence collected from apical planes of the same field. *I*: projected image of EDI anti-Rab10 immunofluorescence collected from the same apical volume as that shown in *B*. *J*: 2× magnified merger of images shown in *H* and *I* shows the colocalization of anti-Rab10 (green) and anti-Sec6 (red) in an apical spot. Scale bars = 10 μm in length.

exocyst interaction in dividing cells. The low-power image shown in Fig. 6*I* shows the characteristic pattern of Sec8 immunofluorescence at cell junctions and apical puncta.

Rab10 binds to a protein complex that includes the Sec8 exocyst protein. Our morphological studies suggest that the mammalian exocyst may interact with Rab10, another mammalian homolog of Sec4p. This interaction was verified in coimmunoprecipitation studies conducted on cells harvested 4 days after reaching confluence, conditions in which we observed the strongest colocalization of Rab10 and Sec8 (Fig. 5). As described in MATERIALS AND METHODS, a postnuclear lysate of MDCK cells was incubated with the EDI Rab10 antibody, and then with protein A-coated beads. Both the supernatant and the eluate were then resolved on gradient gels and immunoblotted with an antibody to Sec8. As shown in Fig. 7*A*, the Sec8 antibody recognized a 110-kDa band consistent with Sec8 in both the supernatant lane and the Rab10-IP lane. Coimmunoprecipitations were conducted with relatively low stringency to enhance sensitivity, resulting in numerous lower molecular weight bands of unknown identity. However, specificity of the immunoprecipitations is demonstrated by the fact that *1*) the Sec8 band is much reduced when the Rab10 antibody is pretreated with a 10× molar excess of immunizing Rab10 peptide and *2*) the Sec8 band occurs only in samples incubated with Rab10 antibody. The fact that the lower molecular width bands recognized by the Sec8 antibody in the supernatant fractions behave similarly to the 110-kDa band suggests that they may be degradation products of Rab10.

The specificity of the Rab10 immunoprecipitation was further confirmed in studies in which a commercial Rab10 antibody obtained from Santa Cruz Life Sciences was used to probe for the presence of Rab10 in the same samples shown in Fig. 7*A*. As shown in Fig. 7*B*, a band running slightly higher than the predicted molecular weight of ~22.5 kDa was de-

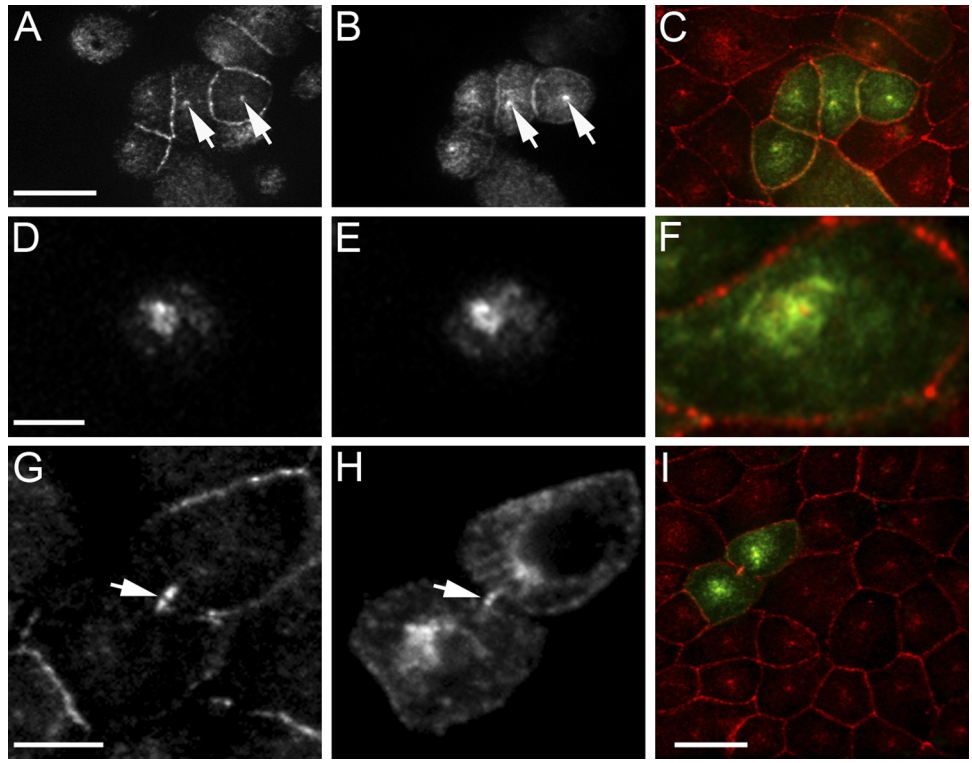

Fig. 6. GFP-Rab10-Q68L colocalizes with Sec8 in apical spots and at abscission sites. *A*: projected image of anti-sec8 immunofluorescence in apical planes of MDCK cells, showing Sec8 at both cell-cell junctions and in single apical spots. *B*: projected image of GFP-Q68L in the same image volume. Arrows indicate examples of colocalization of GFP-Q68L and Sec8 in apical spots. *C*: merged projection of anti-Sec8 (red) and GFP-Q68L (green) from the entire volume of the cells shown in *A* and *B*. *D*: high-magnification image of anti-Sec8 immunofluorescence in apical planes of an MDCK cells. *E*: corresponding image of GFP-Q68L collected from the same volume as *D*, showing colocalization with Sec8 in an apical ring structure. *F*: merged projection of anti-Sec8 (red) and GFP-Q68L (green) from the entire volume of the cells shown in *D* and *E*. *G*: projected image of anti-sec8 immunofluorescence in medial planes of MDCK cells, showing Sec8 at both cell-cell junctions and at the abscission site between 2 daughter cells. *H*: projected image of GFP-Q68L in the same image volume. Arrow indicates colocalization of GFP-Q68L and Sec8 at the abscission site. *I*: low-power merged projection of anti-Sec8 (red) and GFP-Q68L (green) from the entire volume of a field of cells, including those shown in *A* and *B*. Scale bars = 20 μm in length (*A*, *B*, *C*, *I*), 5 μm in length (*D*, *E*, *F*), and 10 μm in length (*G*, *H*).

tected in the sample obtained from lysates incubated with Rab10 antibody, but was much reduced in samples incubated with excess immunizing peptide, and absent from samples incubated without Rab10 antibody. Densitometric analysis of the gel shown in Fig. 7*A* indicates that ~18% of Sec8 is coimmunoprecipitated with Rab10 in this study.

The physical interaction between Rab10 and Sec8 was further verified in reciprocal studies in which protein complexes immunoprecipitated with an antibody to Sec8 were immunoblotted for Rab10 (using the EDI antibody). As shown in Fig. 7*C*, a band corresponding to Rab10 was detected in lysates incubated with antibodies to Sec8. Since Sec8 immunizing peptides were not available for competition studies, control studies were conducted in which cell lysates were incubated with an antibody to N-cadherin, a protein not expected to interact with either Rab10 or Sec8. In this sample, the amount of immunoblotted Rab10 was reduced to nearly that of a sample lacking Sec8 antibodies. As in the previous study, coimmunoprecipitations were conducted with relatively low stringency to enhance sensitivity, resulting in numerous lower molecular weight bands of unknown identity. However, specificity of Rab10 immunoblotting was verified in studies showing that Rab10 was detected in lysates incubated with antibody to Rab10, but was much reduced when Rab10 antibody was pretreated with 10× immunizing peptide. The specificity of the Sec8 immunoprecipitation was confirmed in studies in which a second antibody to Sec8 was used to probe for the presence of Sec8 in the same samples shown in Fig. 7*C*. As shown in Fig. 7*D*, Sec8 is detected in the sample obtained from lysates incubated with antibodies to Sec8, but not in the eluates obtained from lysates lacking Sec8 antibodies, or incubated with an antibody to N-cadherin.

DISCUSSION

The exocyst complex, originally associated with basolateral membrane transport from the TGN of polarized mammalian cells (21, 37, 77), is increasingly appreciated as a general regulator of membrane transport. Various exocyst proteins have since been associated with endocytic recycling (48, 53), insulin-dependent Glut4 translocation (12, 30, 31), plasma membrane remodeling (27, 58, 65, 66, 82), and various centriolar structures (9, 11, 20, 22). The exocyst complex has also been associated with another centriolar structure, the primary cilium. Sec8 and Sec6 have been localized at the base of primary cilia of MDCK cells (55), and Sec10 has been shown to be necessary for ciliogenesis (81). A number of small GTPases have been associated with exocyst-mediated transport in mammalian cells, including Ral (6, 43, 44, 51, 67), Rab11 (20, 48, 80), and ARF6 (20, 53). It has also been suggested that the exocyst serves as an effector for Rab8, a mammalian homolog of the yeast Sec4p protein that mediates transport to the forming bud via interactions with the exocyst complex (23). However, the evidence for this interaction in mammalian cells is circumstantial; Rab8 mediates many of the same pathways associated with the exocyst complex; basolateral membrane transport (2, 28, 29), plasma membrane remodeling (24, 25, 49, 65), insulin-dependent Glut4 traffic (17, 32, 33), and ciliogenesis (16, 42, 46, 79).

Rab10 is another mammalian homolog of Sec4p that is closely related to Rab8 and has likewise been associated with many of the membrane transport pathways mediated by exocyst proteins. Previous studies from our laboratory (3) and others (10, 64) demonstrated that Rab10 mediates basolateral transport in polarized cells and studies of adipocytes also demonstrated that Rab10 is necessary for insulin-dependent

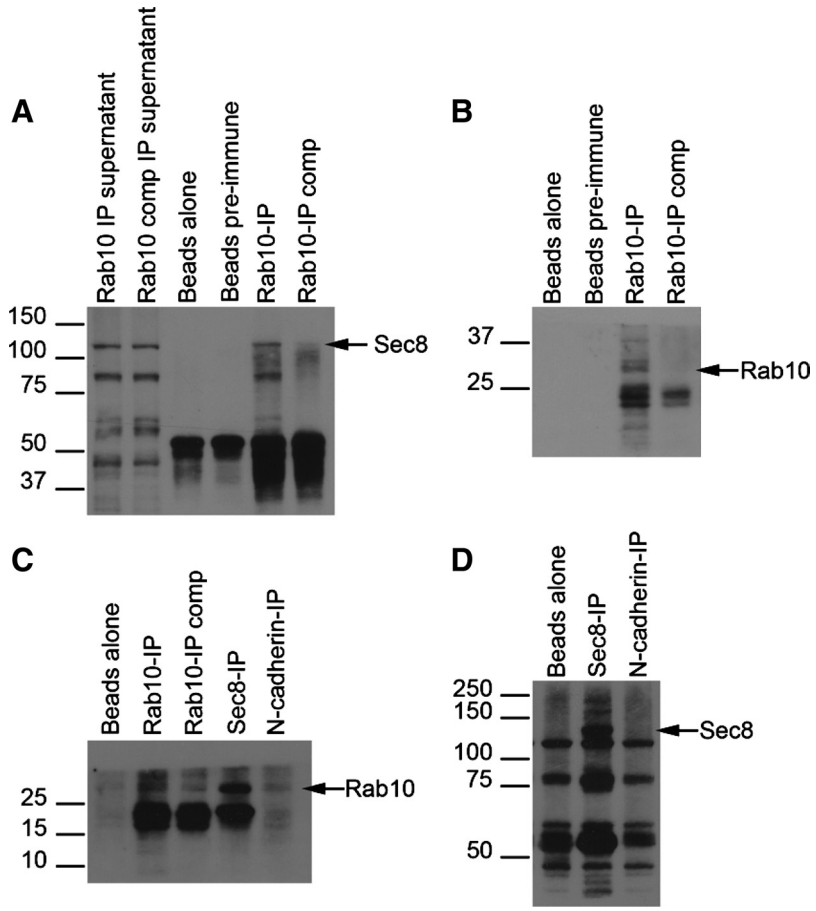

Fig. 7. Rab10 forms a protein complex with Sec8 in MDCK cells. *A*: Sec8 is detected in protein complexes immunoprecipitated with an antibody to Rab10. MDCK cell lysates were incubated with *1*) EDI antibody to Rab10, *2*) preimmune serum, or *3*) EDI antibody after 60-min incubation with a 10-fold molar excess of immunizing peptide. Each sample was then incubated with protein A beads for 30 min. Following magnetic separation of beads, samples were eluted and separated on 4–12% gradient gels. Gels were then probed with antibody to Sec8 and a secondary antibody conjugated to horseradish peroxidase. *Lanes 1* and *2*: proteins in the unbound (supernatant) fraction after incubation of protein A beads with lysate incubated with EDI antibody (*lane 1*) or EDI antibody preincubated with immunizing (competing) peptide (comp; *lane 2*). *Lane 3*: proteins eluted from beads before exposure to cell lysate. *Lane 4*: proteins eluted from beads incubated with lysates that had been preincubated with preimmune serum. *Lane 5*: proteins eluted from beads incubated with lysates that had been preincubated with EDI antibody to Rab10. Note the 110-kDa band consistent with Sec8. *Lane 6*: proteins eluted from beads incubated with lysates that had been preincubated with EDI antibody pretreated with a 10× molar excess of immunizing Rab10 peptide (comp). Note decrease in Sec8 to background levels. Lower molecular weight bands in *lanes 3–6* result from nonspecific binding of the secondary antibody. *B*: confirmatory evidence of Rab10 immunoprecipitation. The same samples described in *A* were immunoblotted with commercial antibody to Rab10 obtained from Santa Cruz Life Sciences. No Rab10 is detected in the samples eluted from beads alone or from beads incubated with lysates that had been incubated with preimmune serum (*lanes 1* and *2*, respectively). Rab10 is detected in the sample eluted from beads incubated with lysates that had been preincubated with antibody to Rab10 (*lane 3*), but not in the sample eluted from beads incubated with lysates that had been preincubated with antibody to Rab10 pretreated with immunizing peptide (*lane 4*). *C*: Rab10 is detected in protein complexes immunoprecipitated with an antibody to Sec8. Studies conducted as described in *A*, except that cell lysates were immunoprecipitated with EDI antibody to Rab10, Sec8, or N-cadherin and gels were probed with Santa Cruz antibody to Rab10. *Lane 1*: proteins eluted from beads before exposure to cell lysate. *Lane 2*: proteins eluted from beads incubated with lysates that had been preincubated with EDI antibody to Rab10. *Lane 3*: proteins eluted from beads incubated with lysates that had been preincubated with EDI antibody to Rab10 pretreated with a 10× molar excess of immunizing peptide. *Lane 4*: proteins eluted from beads incubated with lysate that had been preincubated with antibody to Sec8. Note the ~22.5-kDa band consistent with Rab10. *Lane 5*: proteins eluted from beads incubated with lysates that had been preincubated with antibody to N-cadherin. *D*: confirmatory evidence of Sec8 immunoprecipitation. The same samples described in *C* were immunoblotted with a second antibody to Sec8. No Sec8 is detected in the samples eluted from beads alone or from the eluate obtained from lysate incubated with an antibody to N-cadherin (*lanes 1* and *3*). However, a band consistent with Sec8 is found in bead eluates from lysates preincubated with an antibody to Sec8 (*lane 2*).

translocation of Glut4 transporters to the plasma membrane (13, 59, 60). Here, we demonstrate that Rab10 also associates with primary cilia in mammalian cells. In studies of cultured MDCK and LLC-PK1 cells, antibodies to Rab10 and GFP chimeras of the wild-type and mutant forms of Rab10 were found to localize to primary cilia in ciliated cells and to an apical spot or ring in cells before ciliogenesis. Immunofluorescence studies of rat and mouse tissue demonstrate that Rab10 also associates with cilia in renal epithelia in vivo. In addition, Rab10 colocalizes with Sec8 and Sec6 in apical rings in MDCK cells before ciliogenesis and at the base of nascent cilia. A physical interaction between Rab10 and the exocyst complex was demonstrated in coimmunoprecipitation studies in which Rab10 is detected in protein complexes isolated with an antibody to Sec8, and Sec8 is detected in protein complexes isolated with an antibody to Rab10. While we cannot be certain that the isolated complex reflects interactions occurring at the basal body of the cilium rather than elsewhere in the cell, the

morphological data argue that the predominant interaction between the two occurred in the apical rings of unciliated cells, and at the base of nascent cilia. Consistent with the notion that the apical exocyst serves as an effector for Rab10, we also found an enhanced association of the apical exocyst with the GTPase-defective GFP-Rab10-Q68L. A similar enhanced accumulation at the cilium base was observed for the GTPase-defective form of Rab8, Rab8-Q67L (46).

In general, GFP-Rab10 showed a more limited distribution on cilia compared with endogenous Rab10, as detected by immunofluorescence. Whereas immunofluorescence detects Rab10 at both the base of the cilium as well as along the entire extent of the axoneme, GFP-Rab10 is typically found only at the base of the cilium. We doubt that this reflects a steric problem of GFP access to the cilium shaft as GFP-Rab8 has previously been found to access the entire length of the cilium (46), and we found a similarly limited distribution of exogenously expressed FLAG-Rab10. Rather, the limited distribution of GFP-Rab10 may result from our transient expression system in which the duration of GFP-Rab10 expression is somewhat shorter than the period of ciliogenesis. Because of this, expression of GFP-Rab10 may be waning by the time a cell has fully developed a cilium, and thus fail to reflect the steady-state distribution of Rab10. Consistent with this, we find relatively low levels of GFP-Rab10 expression in older cultures with fully formed cilia.

The colocalization of Rab10 and exocyst proteins at the apparent site of cilium formation, and at the basal body of nascent cilia, suggests that Rab10 may function in the process of ciliogenesis. However, studies not shown here, designed to test the role of Rab10 in ciliogenesis, were inconclusive. In some studies, cilia were formed less frequently in cells transiently expressing shRNA targeting Rab10 or Rab10-Q68L, a mutant that had previously been shown to alter Rab10 function in endocytosis, TGN transport, and Glut4 trafficking (3, 59, 64), relative to untransfected cells, or cells expressing GFP-Rab10 or GFP-Rab7. However, the effects were not consistent. The lack of consistency may result from the transient expression system, whose timeframe coincides with that of ciliogenesis, and thus may frequently fail to achieve sufficient expression of mutant Rab10 or downregulation of endogenous Rab10 before ciliogenesis.

The lack of consistent, robust effects of Rab10 manipulations on ciliogenesis may also reflect the complexity of a membrane transport system mediated by exocyst proteins and multiple Rab proteins that interact with one another via multiple shared factors. Both Rab10 and Rab8 have been identified as substrates for AS160 (32, 41, 59) and MSS4 (7, 34). Proteomic analysis also determined that Rab10 and Rab8 interact with the same protein complexes (18). A recent study indicates that Rab11 also participates in ciliogenesis, via an interaction with Rabin8 (35, 74), a Rab8 GEF (26). Rab8, Rab10, and Rab11 all interact with myosin Va and Vb (57). Finally, Rab11 has been demonstrated to interact with Sec15 (48, 80), the exocyst subunit that would be expected to interact directly with Rab8 and Rab10. These multiple shared interactions may complicate interpretation of studies involving manipulation of Rab10 alone. Indeed, in one previous study, the effects of Rab10 downregulation on basolateral membrane transport were not apparent, requiring simultaneous downregulation of Rab8 and expression of an inactive form of Rab10 (64). Studies of insulin-dependent Glut4 translocation likewise indicate that Rab8 and Rab10 have overlapping functions, although in this case they are differentially regulated in different cell types such that Glut4 traffic is mediated by Rab10 in adipocytes (59, 60), but by Rab8 in muscle cells (32, 33).

The mammalian exocyst has been found to mediate a diverse array of membrane transport processes, many of which are associated with different stages in the cell cycle and development of the polarized epithelial phenotype. Exocyst proteins have been associated with membrane transport to the leading edge of migrating cells (58, 66, 82), to the abscission sites of dividing cells (9, 11, 20, 22), to the basal body during ciliogenesis (55, 81), and to the basolateral plasma membrane (21, 76, 77) and the apical plasma membrane (48) of polarized cells.

The mechanism by which the exocyst mediates these diverse functions is likely to be based on differences in the molecular constitution of the exocyst complex associated with each. In this sense, the term "exocyst complex" is misleading, in that there is excellent evidence that mammalian exocyst complexes exist in many forms (1, 44, 69, 76, 77). It is also likely that the functional specificity of different exocyst complexes is mediated by their associations with different combinations of Rab proteins and their associated regulators. In this regard, it may be significant that the functions of various Rab proteins associated with the exocyst likewise vary according to differentiation/cell cycle stage. Rab8 has been associated with transport to the leading edge of migrating cells (24, 25, 49), to the primary cilium during ciliogenesis (15, 16, 42, 46, 74, 79), and to the basolateral plasma membrane in polarized cells (2, 28, 29). Rab11 mediates transport to the leading edge of migrating cells (19, 39, 52, 78), transport to abscission sites of dividing cells (20, 73), transport to the apical plasma membrane of polarized cells (5, 8, 36, 72) and has recently been associated with ciliogenesis (35, 74). The functions of Rab10 likewise appear to depend on differentiation/cell cycle. Rab10 mediates transport from the TGN to the basolateral membrane during the development of polarity (64) and basolateral endocytic recycling in polarized cells (3). Here, we show that Rab10 also associates with primary cilia in quiescent cells, with the basal body during ciliogenesis, and with abscission sites in dividing cells. In studies not shown here, we also found that Rab10 localizes to spindle poles in dividing cells. The association of Rab10 with centrosomal structures across a range of different cell cycle stages suggests that Rab10 may be centrally involved in differentiation and/or cell cycle progression. In this regard, it is intriguing that Rab10 has been found to interact with Aurora kinase A (18), a protein involved in the disassembly of the primary cilium that precedes (and perhaps cues) entry into the cell cycle (50, 54).

The diverse functions, molecular constitutions, and molecular interactions of the different exocyst functions complicate dissecting the molecular mechanism of any one exocyst-mediated pathway. However, one strategy for identifying the proteins associated with a particular pathway will be to isolate exocyst complexes from cells at a particular stage of the cell cycle, or via protein interactions that are associated with one particular pathway. In this regard, the predominant accumulation of Rab10, and particularly Rab10-Q68L, at the basal body of nascent cilia may be useful for isolating and thus identifying the constituents of the basal body exocyst complex. These studies are thus likely to yield insights into the molecular

mechanism of membrane transport to the primary cilium, a process that is fundamentally important to cell signaling, development, and a variety of human diseases.

GRANTS

This work was supported by the National Institutes of Health (R01-DK-51098 to K. Dunn, R01-DK-050141 to R. Bacallao) and the Dialysis Clinic (K. Dunn). Microscopy studies were conducted at the Indiana Center for Biological Microscopy.

DISCLOSURES

No conflicts of interest, financial or otherwise, are declared by the author(s).

REFERENCES

1. **Andersen NJ, Yeaman C.** Sec3-containing exocyst complex is required for desmosome assembly in mammalian epithelial cells. *Mol Biol Cell* 21: 152–164, 2010.
2. **Ang AL, Folsch H, Koivisto UM, Pypaert M, Mellman I.** The Rab8 GTPase selectively regulates AP-1B-dependent basolateral transport in polarized Madin-Darby canine kidney cells. *J Cell Biol* 163: 339–350, 2003.
3. **Babbey CM, Ahktar N, Wang E, Chen CC, Grant BD, Dunn KW.** Rab10 regulates membrane transport through early endosomes of polarized Madin-Darby canine kidney cells. *Mol Biol Cell* 17: 3156–3175, 2006.
4. **Berbari NF, Lewis JS, Bishop GA, Askwith CC, Mykytyn K.** Bardet-Biedl syndrome proteins are required for the localization of G protein-coupled receptors to primary cilia. *Proc Natl Acad Sci USA* 105: 4242–4246, 2008.
5. **Brown PS, Wang E, Aroeti B, Chapin SJ, Mostov KE, Dunn KW.** Definition of distinct compartments in polarized Madin-Darby canine kidney (MDCK) cells for membrane-volume sorting, polarized sorting and apical recycling. *Traffic* 1: 124–140, 2000.
6. **Brymora A, Valova VA, Larsen MR, Roufogalis BD, Robinson PJ.** The brain exocyst complex interacts with RalA in a GTP-dependent manner: identification of a novel mammalian Sec3 gene and a second Sec15 gene. *J Biol Chem* 276: 29792–29797, 2001.
7. **Burton JL, Burns ME, Gatti E, Augustine GJ, De Camilli P.** Specific interactions of Mss4 with members of the Rab GTPase subfamily. *EMBO J* 13: 5547–5558, 1994.
8. **Casanova JE, Wang X, Kumar R, Bhartur SG, Navarre J, Woodrum JE, Altschuler Y, Ray GS, Goldenring JR.** Association of Rab25 and Rab11a with the apical recycling system of polarized Madin-Darby canine kidney cells. *Mol Biol Cell* 10: 47–61, 1999.
9. **Cascone I, Selimoglu R, Ozdemir C, Del Nery E, Yeaman C, White M, Camonis J.** Distinct roles of RalA and RalB in the progression of cytokinesis are supported by distinct RalGEFs. *EMBO J* 27: 2375–2387, 2008.
10. **Chen CC, Schweinsberg PJ, Vashist S, Mareiniss DP, Lambie EJ, Grant BD.** RAB-10 is required for endocytic recycling in the *Caenorhabditis elegans* intestine. *Mol Biol Cell* 17: 1286–1297, 2006.
11. **Chen XW, Inoue M, Hsu SC, Saltiel AR.** RalA-exocyst-dependent recycling endosome trafficking is required for the completion of cytokinesis. *J Biol Chem* 281: 38609–38616, 2006.
12. **Chen XW, Leto D, Chiang SH, Wang Q, Saltiel AR.** Activation of RalA is required for insulin-stimulated Glut4 trafficking to the plasma membrane via the exocyst and the motor protein Myo1c. *Dev Cell* 13: 391–404, 2007.
13. **Chen Y, Deng Y, Zhang J, Yang L, Xie X, Xu T.** GDI-1 preferably interacts with Rab10 in insulin-stimulated GLUT4 translocation. *Biochem J* 422: 229–235, 2009.
14. **Corbit KC, Aanstad P, Singla V, Norman AR, Stainier DY, Reiter JF.** Vertebrate Smoothened functions at the primary cilium. *Nature* 437: 1018–1021, 2005.
15. **Deretic D.** Rab proteins and post-Golgi trafficking of rhodopsin in photoreceptor cells. *Electrophoresis* 18: 2537–2541, 1997.
16. **Deretic D, Huber LA, Ransom N, Mancini M, Simons K, Papermaster DS.** Rab8 in retinal photoreceptors may participate in rhodopsin transport and in rod outer segment disk morphogenesis. *J Cell Sci* 108: 215–224, 1995.
17. **Dugani CB, Klip A.** Glucose transporter 4: cycling, compartments and controversies. *EMBO Rep* 6: 1137–1142, 2005.
18. **Ewing RM, Chu P, Elisma F, Li H, Taylor P, Climie S, McBroom-Cerajewski L, Robinson MD, O'Connor L, Li M, Taylor R, Dharsee M, Ho Y, Heilbut A, Moore L, Zhang S, Ornatsky O, Bukhman YV, Ethier M, Sheng Y, Vasilescu J, Abu-Farha M, Lambert JP, Duewel HS, Stewart II, Kuehl B, Hogue K, Colwill K, Gladwish K, Muskat B, Kinach R, Adams SL, Moran MF, Morin GB, Topaloglou T, Figeys D.** Large-scale mapping of human protein-protein interactions by mass spectrometry. *Mol Syst Biol* 3: 89, 2007.
19. **Fan GH, Lapierre LA, Goldenring JR, Sai J, Richmond A.** Rab11-family interacting protein 2 and myosin Vb are required for CXCR2 recycling and receptor-mediated chemotaxis. *Mol Biol Cell* 15: 2456–2469, 2004.
20. **Fielding AB, Schonteich E, Matheson J, Wilson G, Yu X, Hickson GR, Srivastava S, Baldwin SA, Prekeris R, Gould GW.** Rab11-FIP3 and FIP4 interact with Arf6 and the exocyst to control membrane traffic in cytokinesis. *EMBO J* 24: 3389–3399, 2005.
21. **Grindstaff KK, Yeaman C, Anandasabapathy N, Hsu SC, Rodriguez-Boulan E, Scheller RH, Nelson WJ.** Sec6/8 complex is recruited to cell-cell contacts and specifies transport vesicle delivery to the basal-lateral membrane in epithelial cells. *Cell* 93: 731–740, 1998.
22. **Gromley A, Yeaman C, Rosa J, Redick S, Chen CT, Mirabelle S, Guha M, Sillibourne J, Doxsey SJ.** Centriolin anchoring of exocyst and SNARE complexes at the midbody is required for secretory vesicle-mediated abscission. *Cell* 123: 75–87, 2005.
23. **Guo W, Roth D, Walch-Solimena C, Novick P.** The exocyst is an effector for Sec4p, targeting secretory vesicles to sites of exocytosis. *EMBO J* 18: 1071–1080, 1999.
24. **Hattula K, Furuhjelm J, Arffman A, Peranen J.** A Rab8-specific GDP/GTP exchange factor is involved in actin remodeling and polarized membrane transport. *Mol Biol Cell* 13: 3268–3280, 2002.
25. **Hattula K, Furuhjelm J, Tikkanen J, Tanhuanpaa K, Laakkonen P, Peranen J.** Characterization of the Rab8-specific membrane traffic route linked to protrusion formation. *J Cell Sci* 119: 4866–4877, 2006.
26. **Hattula K, Peranen J.** Purification and functional properties of a Rab8-specific GEF (Rabin3) in action remodeling and polarized transport. *Methods Enzymol* 403: 284–295, 2005.
27. **Hazuka CD, Foletti DL, Hsu SC, Kee Y, Hopf FW, Scheller RH.** The sec6/8 complex is located at neurite outgrowth and axonal synapse-assembly domains. *J Neurosci* 19: 1324–1334, 1999.
28. **Henry L, Sheff DR.** Rab8 regulates basolateral secretory, but not recycling, traffic at the recycling endosome. *Mol Biol Cell* 19: 2059–2068, 2008.
29. **Huber LA, Pimplikar S, Parton RG, Virta H, Zerial M, Simons K.** Rab8, a small GTPase involved in vesicular traffic between the TGN and the basolateral plasma membrane. *J Cell Biol* 123: 35–45, 1993.
30. **Inoue M, Chang L, Hwang J, Chiang SH, Saltiel AR.** The exocyst complex is required for targeting of Glut4 to the plasma membrane by insulin. *Nature* 422: 629–633, 2003.
31. **Inoue M, Chiang SH, Chang L, Chen XW, Saltiel AR.** Compartmentalization of the exocyst complex in lipid rafts controls Glut4 vesicle tethering. *Mol Biol Cell* 17: 2303–2311, 2006.
32. **Ishikura S, Bilan PJ, Klip A.** Rabs 8A and 14 are targets of the insulin-regulated Rab-GAP AS160 regulating GLUT4 traffic in muscle cells. *Biochem Biophys Res Commun* 353: 1074–1079, 2007.
33. **Ishikura S, Klip A.** Muscle cells engage Rab8A and myosin Vb in insulin-dependent GLUT4 translocation. *Am J Physiol Cell Physiol* 295: C1016–C1025, 2008.
34. **Itzen A, Pylypenko O, Goody RS, Alexandrov K, Rak A.** Nucleotide exchange via local protein unfolding–structure of Rab8 in complex with MSS4. *EMBO J* 25: 1445–1455, 2006.
35. **Knodler A, Feng S, Zhang J, Zhang X, Das A, Peranen J, Guo W.** Coordination of Rab8 and Rab11 in primary ciliogenesis. *Proc Natl Acad Sci USA* 107: 6346–6351, 2010.
36. **Lapierre LA, Avant KM, Caldwell CM, Ham AJ, Hill S, Williams JA, Smolka AJ, Goldenring JR.** Characterization of immunoisolated human gastric parietal cells tubulovesicles: identification of regulators of apical recycling. *Am J Physiol Gastrointest Liver Physiol* 292: G1249–G1262, 2007.
37. **Lipschutz JH, Guo W, O'Brien LE, Nguyen YH, Novick P, Mostov KE.** Exocyst is involved in cystogenesis and tubulogenesis and acts by modulating synthesis and delivery of basolateral plasma membrane and secretory proteins. *Mol Biol Cell* 11: 4259–4275, 2000.

38. **Liu Q, Tan G, Levenkova N, Li T, Pugh EN Jr, Rux JJ, Speicher DW, Pierce EA.** The proteome of the mouse photoreceptor sensory cilium complex. *Mol Cell Proteomics* 6: 1299–1317, 2007.
39. **Mammoto A, Ohtsuka T, Hotta I, Sasaki T, Takai Y.** Rab11BP/Rabphilin-11, a downstream target of rab11 small G protein implicated in vesicle recycling. *J Biol Chem* 274: 25517–25524, 1999.
40. **Marshall WF.** The cell biological basis of ciliary disease. *J Cell Biol* 180: 17–21, 2008.
41. **Miinea CP, Sano H, Kane S, Sano E, Fukuda M, Peranen J, Lane WS, Lienhard GE.** AS160, the Akt substrate regulating GLUT4 translocation, has a functional Rab GTPase-activating protein domain. *Biochem J* 391: 87–93, 2005.
42. **Moritz OL, Tam BM, Hurd LL, Peranen J, Deretic D, Papermaster DS.** Mutant rab8 Impairs docking and fusion of rhodopsin-bearing post-Golgi membranes and causes cell death of transgenic Xenopus rods. *Mol Biol Cell* 12: 2341–2351, 2001.
43. **Moskalenko S, Henry DO, Rosse C, Mirey G, Camonis JH, White MA.** The exocyst is a Ral effector complex. *Nat Cell Biol* 4: 66–72, 2002.
44. **Moskalenko S, Tong C, Rosse C, Mirey G, Formstecher E, Daviet L, Camonis J, White MA.** Ral GTPases regulate exocyst assembly through dual subunit interactions. *J Biol Chem* 278: 51743–51748, 2003.
45. **Munson M, Novick P.** The exocyst defrocked, a framework of rods revealed. *Nat Struct Mol Biol* 13: 577–581, 2006.
46. **Nachury MV, Loktev AV, Zhang Q, Westlake CJ, Peranen J, Merdes A, Slusarski DC, Scheller RH, Bazan JF, Sheffield VC, Jackson PK.** A core complex of BBS proteins cooperates with the GTPase Rab8 to promote ciliary membrane biogenesis. *Cell* 129: 1201–1213, 2007.
47. **Nauli SM, Alenghat FJ, Luo Y, Williams E, Vassilev P, Li X, Elia AE, Lu W, Brown EM, Quinn SJ, Ingber DE, Zhou J.** Polycystins 1 and 2 mediate mechanosensation in the primary cilium of kidney cells. *Nat Genet* 33: 129–137, 2003.
48. **Oztan A, Silvis M, Weisz OA, Bradbury NA, Hsu SC, Goldenring JR, Yeaman C, Apodaca G.** Exocyst requirement for endocytic traffic directed toward the apical and basolateral poles of polarized MDCK cells. *Mol Biol Cell* 18: 3978–3992, 2007.
49. **Peranen J, Auvinen P, Virta H, Wepf R, Simons K.** Rab8 promotes polarized membrane transport through reorganization of actin and microtubules in fibroblasts. *J Cell Biol* 135: 153–167, 1996.
50. **Plotnikova OV, Golemis EA, Pugacheva EN.** Cell cycle-dependent ciliogenesis and cancer. *Cancer Res* 68: 2058–2061, 2008.
51. **Polzin A, Shipitsin M, Goi T, Feig LA, Turner TJ.** Ral-GTPase influences the regulation of the readily releasable pool of synaptic vesicles. *Mol Cell Biol* 22: 1714–1722, 2002.
52. **Powelka AM, Sun J, Li J, Gao M, Shaw LM, Sonnenberg A, Hsu VW.** Stimulation-dependent recycling of integrin beta1 regulated by ARF6 and Rab11. *Traffic* 5: 20–36, 2004.
53. **Prigent M, Dubois T, Raposo G, Derrien V, Tenza D, Rosse C, Camonis J, Chavrier P.** ARF6 controls postendocytic recycling through its downstream exocyst complex effector. *J Cell Biol* 163: 1111–1121, 2003.
54. **Pugacheva EN, Jablonski SA, Hartman TR, Henske EP, Golemis EA.** HEF1-dependent Aurora A activation induces disassembly of the primary cilium. *Cell* 129: 1351–1363, 2007.
55. **Rogers KK, Wilson PD, Snyder RW, Zhang X, Guo W, Burrow CR, Lipschutz JH.** The exocyst localizes to the primary cilium in MDCK cells. *Biochem Biophys Res Commun* 319: 138–143, 2004.
56. **Rohatgi R, Milenkovic L, Scott MP.** Patched1 regulates hedgehog signaling at the primary cilium. *Science* 317: 372–376, 2007.
57. **Roland JT, Lapierre LA, Goldenring JR.** Alternative splicing in class V myosins determines association with Rab10. *J Biol Chem* 284: 1213–1223, 2009.
58. **Rosse C, Hatzoglou A, Parrini MC, White MA, Chavrier P, Camonis J.** RalB mobilizes the exocyst to drive cell migration. *Mol Cell Biol* 26: 727–734, 2006.
59. **Sano H, Eguez L, Teruel MN, Fukuda M, Chuang TD, Chavez JA, Lienhard GE, McGraw TE.** Rab10, a target of the AS160 Rab GAP, is required for insulin-stimulated translocation of GLUT4 to the adipocyte plasma membrane. *Cell Metab* 5: 293–303, 2007.
60. **Sano H, Roach WG, Peck GR, Fukuda M, Lienhard GE.** Rab10 in insulin-stimulated GLUT4 translocation. *Biochem J* 411: 89–95, 2008.
61. **Satir P, Christensen ST.** Overview of structure and function of mammalian cilia. *Annu Rev Physiol* 69: 377–400, 2007.
62. **Schneider L, Clement CA, Teilmann SC, Pazour GJ, Hoffmann EK, Satir P, Christensen ST.** PDGFRαα signaling is regulated through the primary cilium in fibroblasts. *Curr Biol* 15: 1861–1866, 2005.
63. **Scholey JM.** Intraflagellar transport motors in cilia: moving along the cell's antenna. *J Cell Biol* 180: 23–29, 2008.
64. **Schuck S, Gerl MJ, Ang A, Manninen A, Keller P, Mellman I, Simons K.** Rab10 is involved in basolateral transport in polarized Madin-Darby canine kidney cells. *Traffic* 8: 47–60, 2007.
65. **Simons M, Saffrich R, Reiser J, Mundel P.** Directed membrane transport is involved in process formation in cultured podocytes. *J Am Soc Nephrol* 10: 1633–1639, 1999.
66. **Spiczka KS, Yeaman C.** Ral-regulated interaction between Sec5 and paxillin targets exocyst to focal complexes during cell migration. *J Cell Sci* 121: 2880–2891, 2008.
67. **Sugihara K, Asano S, Tanaka K, Iwamatsu A, Okawa K, Ohta Y.** The exocyst complex binds the small GTPase RalA to mediate filopodia formation. *Nat Cell Biol* 4: 73–78, 2002.
68. **Torkko JM, Manninen A, Schuck S, Simons K.** Depletion of apical transport proteins perturbs epithelial cyst formation and ciliogenesis. *J Cell Sci* 121: 1193–1203, 2008.
69. **Vik-Mo EO, Oltedal L, Hoivik EA, Kleivdal H, Eidet J, Davanger S.** Sec6 is localized to the plasma membrane of mature synaptic terminals and is transported with secretogranin II-containing vesicles. *Neuroscience* 119: 73–85, 2003.
70. **Wang E, Brown PS, Aroeti B, Chapin SJ, Mostov KE, Dunn KW.** Apical and basolateral endocytic pathways of MDCK cells meet in acidic common endosomes distinct from a nearly neutral apical recycling endosome. *Traffic* 1: 480–493, 2000.
71. **Wang E, Pennington JG, Goldenring JR, Hunziker W, Dunn KW.** Brefeldin A rapidly disrupts plasma membrane polarity by blocking polar sorting in common endosomes of MDCK cells. *J Cell Sci* 114: 3309–3321, 2001.
72. **Wang X, Kumar R, Navarre J, Casanova JE, Goldenring JR.** Regulation of vesicle trafficking in Madin-Darby canine kidney cells by Rab11a and Rab25. *J Biol Chem* 275: 29138–29146, 2000.
73. **Westlake CJ, Junutula JR, Simon GC, Pilli M, Prekeris R, Scheller RH, Jackson PK, Eldridge AG.** Identification of Rab11 as a small GTPase binding protein for the Evi5 oncogene. *Proc Natl Acad Sci USA* 104: 1236–1241, 2007.
74. **Westlake CJ, Scheller RH, Jackson PK, Nachury MV.** A Rab11/Rab8 switch regulates membrane transport to nascent primary cilia. *Mol Biol Cell* 19: 2546a, 2008.
75. **Yamashiro DJ, Tycko B, Fluss SR, Maxfield FR.** Segregation of transferrin to a mildly acidic (pH 6.5) para-Golgi compartment in the recycling pathway. *Cell* 37: 789–800, 1984.
76. **Yeaman C, Grindstaff KK, Nelson WJ.** Mechanism of recruiting Sec6/8 (exocyst) complex to the apical junctional complex during polarization of epithelial cells. *J Cell Sci* 117: 559–570, 2004.
77. **Yeaman C, Grindstaff KK, Wright JR, Nelson WJ.** Sec6/8 complexes on *trans*-Golgi network and plasma membrane regulate late stages of exocytosis in mammalian cells. *J Cell Biol* 155: 593–604, 2001.
78. **Yoon SO, Shin S, Mercurio AM.** Hypoxia stimulates carcinoma invasion by stabilizing microtubules and promoting the Rab11 trafficking of the alpha6beta4 integrin. *Cancer Res* 65: 2761–2769, 2005.
79. **Yoshimura S, Egerer J, Fuchs E, Haas AK, Barr FA.** Functional dissection of Rab GTPases involved in primary cilium formation. *J Cell Biol* 178: 363–369, 2007.
80. **Zhang XM, Ellis S, Sriratana A, Mitchell CA, Rowe T.** Sec15 is an effector for the Rab11 GTPase in mammalian cells. *J Biol Chem* 279: 43027–43034, 2004.
81. **Zuo X, Guo W, Lipschutz JH.** The exocyst protein Sec10 is necessary for primary ciliogenesis and cystogenesis in vitro. *Mol Biol Cell* 20: 2522–2529, 2009.
82. **Zuo X, Zhang J, Zhang Y, Hsu SC, Zhou D, Guo W.** Exo70 interacts with the Arp2/3 complex and regulates cell migration. *Nat Cell Biol* 8: 1383–1388, 2006.